Flow of drops immersed in a liquid phase through capillary tubes

Sygifredo Cobos, sygifredo@rdc.puc-rio.br
Márcio da Silveira Carvalho, msc@rdc.puc-rio.br
PUC-Rio. Dpto. Eng Mecânica. Rua Marquês de São Vicente, 225 Gávea.

Vladimir Alvarado, valvarad@uwyo.edu
Department of Chemical and Petroleum Engineering. University of Wyoming. Laramie, WY.

Abstract. *Flow of emulsions is found in many petroleum recovery and production processes and it is often referred to in the context of tertiary oil recovery. The flow of emulsions in porous media depends upon factors as medium drop size to pore size distribution ratio, viscosity ratio, flow rate and the effect of these parameters is far from being entirely understood. A detailed analysis at microscopic scale of the flow phenomena involved is essential for the better understanding of the flow of an emulsion in a reservoir. This would lead to the development of better simulation models, henceforth increasing the predictability capability of reservoir simulators for EOR applications. In this work a theoretical analysis for the flow of a single drop through a capillary was done by solving the Navier-Stokes equations with the appropriate boundary conditions for free-surface flow and solving the system of equations by Galerkin's method and finite element basis functions. The study is compared with experimental data available in literature and shows a good agreement. Results show the effect of the viscosity ratio and capillary number on the flow and can be used as initial condition for predicting the liquid-liquid flow in a capillary with a constriction.*

Keywords: *enhanced oil recovery, emulsions, capillary, porous media, immiscible displacement.*

1. INTRODUCTION

Flow of emulsions is found in many petroleum recovery and production processes and it is often referred to in the context of tertiary oil recovery. Evaluating enhanced oil recovery methods depends on understanding multiphase flow through the porous matrix.

To understand how emulsions flows in porous media, it is important to analyze the flow of liquid drops immersed in a liquid phase through capillaries. Presence of the liquid-liquid interface strongly affects the multiphase flow in porous media. The important parameter of this class of flow are the viscosity ratio, capillary number, drop size to pore size distribution ratio has to be analyzed. A broad review of the current state of emulsion flow in porous media is presented by Jansen (2001).

If the sizes of the oil drops moving through the porous media are in the order of the pore size, we are dealing with drop flow. Perhaps the simple possible representation of a multiphase flow in a small pore is the pressure-driven flow of a liquid containing a freely suspended and deformable drop through a channel. A comprehensive review on this subject was presented by Olbricht (1996).

Most of the related work found in the literature for immiscible displacement of a liquid in a capillary tube deals with the case of a gas displacing a viscous liquid, going back to the first works of Fairbrother and Stubbs (1935) and Taylor (1960). In the experiments reported in these works, the Reynolds number was kept small enough to assure negligible inertial effects. In the work of Taylor, measurements of the amount of liquid left behind when a viscous liquid is blown from an open ended tube are presented. The mass (m) of the liquid left on the wall can be written as a function of the velocity of the tip of the interface (U) and the mean velocity ($\overline{U}$) of the liquid ahead of the gas-liquid interface,

$$\frac{U_b - \overline{U}}{U_b} = m \tag{1}$$

Taylor (1960) studied the dependence of the mass fraction on the capillary number $Ca \equiv \frac{\mu U}{\sigma}$ and presents a rough sketch of possible streamlines for different values of m.

The case of liquid-liquid displacement is less studied in the literature. One of these works is presented by Goldsmith and Mason (1968), who studied the flow and deformation of single large liquid bubble suspended in liquids undergoing laminar flow through circular tubes. They report experimental results for the thickness of the liquid film surrounding bubbles and determined by direct observation through a microscope, as report too the film thickness calculated through:

$$\frac{U_b - \overline{U}}{U_b} = \frac{2h}{R}(1 - \frac{2h}{R}) \tag{2}$$

The results showed that the film thickness rises as viscosity ratio $\lambda = \frac{\mu_1}{\mu_2}$ is increased, where the index 1 refers to the displacing fluid and 2, to the displaced fluid.

Soares et al. (2005) presented a theoretycal analysis of liquid-liquid immiscible displacement in capillaries using the finite element method to solve the governing equations. They analized a liquid being displaced by a less viscous liquid.

In this work, the steady displacement of a viscous liquid by a long drop of another viscous liquid in a capillary tube is analyzed by a theory approach consisted on solving the governing equations of this free surface problem using the finite element method. The flow field variables and the position of the interface between the two liquids are all solved simultaneously. The theoretical predictions show the effect of different parameters on the interface configuration and on the thickness of the layer of the displaced liquid left on the walls and the pressure gradient along the capillary. The results presented here extend those presented by Soares et al (2005) to cases where the drop viscosity is higher than the viscosity of the continuous phase. This condition is more appropiate to study the flow of an oil-water emulsion through a capillary.

2. MATHEMATICAL FORMULATION

The physical model to describe the displacement of a Newtonian liquid of viscosity μ_2 by a long drop of a second Newtonian liquid of viscosity μ_1 is presented in this section. The displacing drop (Liquid 1) is translating steadily with speed (**U**). To simplify the analysis, the governing equations are written with respect to a moving frame of reference located at the tip of the interface. In this frame of reference, the flow is steady and the walls are moving with velocity (**U**).

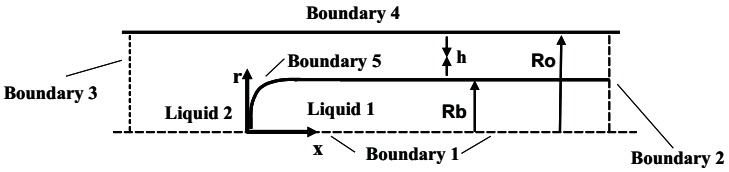

Figure 1. Schematics of the problem.

The geometry analyzed is an axisymmetric capillary of radius **Ro** (Fig. 1). The liquids are assumed to be incompressible, and the flow is laminar and inertialess. The velocity and pressure fields are governed by the continuity and momentum equations. In cylindrical coordinates, these governing equations are written as (the subscript k = 1, 2 labels the two liquids):

$$0 = \frac{1}{r}\frac{\partial}{\partial r}(rv_k) + \frac{\partial}{\partial x}(u_k) \tag{3}$$

$$\rho_k\left(v_k\frac{\partial u_k}{\partial r} + u_k\frac{\partial u_k}{\partial x}\right) = \left[\frac{1}{r}\frac{\partial}{\partial r}(r\tau_{(rx)k}) + \frac{\partial}{\partial x}(\tau_{(xx)k})\right] - \frac{\partial p_k}{\partial x} \tag{4}$$

$$\rho_k\left(v_k\frac{\partial v_k}{\partial r} + u_k\frac{\partial v_k}{\partial x}\right) = \left[\frac{1}{r}\frac{\partial}{\partial r}(r\tau_{(rr)k}) - \frac{\tau_{\theta\theta}}{r} + \frac{\partial}{\partial x}(\tau_{(rx)k})\right] - \frac{\partial p_k}{\partial r} \tag{5}$$

In these equations, x and r are the axial and radial coordinates, u and v are the axial and radial components of the velocity vector ($\mathbf{u} = u\hat{\mathbf{e}}x + v\hat{\mathbf{e}}r$), p is the pressure, $\tau_{xx}, \tau_{xr}, \tau_{rx}, \tau_{rr}$, and τ_{uu} are components of the extra-stress tensor, $\tau(\tau \equiv \mathbf{T} + p\mathbf{I})$, where T is the stress tensor and I is the unit tensor.

The extra-stress tensor τ is proportional to the rate-of-deformation tensor:

$$\tau_{\mathbf{k}} = \mu_{\mathbf{k}}\dot{\gamma} \tag{6}$$

$$\dot{\gamma} = (\nabla\mathbf{u} + \nabla\mathbf{u}^{\mathbf{T}}) \tag{7}$$

Far enough upstream of the interface (Boundary 3) the flow is assumed to be fully developed and hence the pressure is uniform on the cross section:

$$\mathbf{n}\cdot\nabla\mathbf{u_2} = \mathbf{0} \quad , \quad \mathrm{p}_1 = p_{in} \tag{8}$$

Where **n** is the unit vector normal to the boundary and p_{in} is a constant. Far enough downstream of the interface (Boundary 2), the flow is also assumed to be fully developed, but the pressure is not imposed:

$$\mathbf{n}\cdot\nabla\mathbf{u_1} = \mathbf{0} \quad , \quad \mathbf{n}\cdot\nabla\mathbf{u_2} = \mathbf{0} \tag{9}$$

The symmetry axis Boundary 1 is a streamline of the flow, and there the shear stress vanishes:

$$\mathbf{n}\cdot\mathbf{u} = \mathbf{0} \quad , \quad \mathbf{t}\cdot(\mathbf{n}\cdot\mathbf{T}) = \mathbf{0} \tag{10}$$

where **t** is the unit vector tangent to the boundary. The no-slip and impermeability conditions are applied along the tube wall (Boundary 4):

$$\mathbf{u} = U\mathbf{e}_x \tag{11}$$

The liquid-liquid interface (Boundary 5) is also a streamline of the flow. There is no velocity jump, while a normal stress jump occurs at the interface, which is balanced by the capillary pressure:

$$\mathbf{n} \cdot (\mathbf{u_1} - \mathbf{u_2}) = \mathbf{0} \tag{12}$$

$$\mathbf{n} \cdot (p_1 - p_2) + \mathbf{n} \cdot (\tau_1 - \tau_2) = \frac{\sigma}{R_m}\eta \tag{13}$$

Where $1/R_m$ is the local mean curvature of the interface, given by:

$$\frac{1}{R_m}\mathbf{n} = \frac{\mathbf{1}}{\sqrt{\mathbf{x_s^2} + \mathbf{r_s^2}}}\frac{\partial \mathbf{t}}{\partial \mathbf{s}} - \frac{\mathbf{x_s}}{\mathbf{r}\sqrt{\mathbf{x_s^2} + \mathbf{r_s^2}}}\mathbf{n} \tag{14}$$

and s is the arc-lenght curvilinear coordinate along the interface.
The relevant dimensionless parameters are:

$$Capillary Number : Ca \equiv \frac{\mu_2 U}{\sigma} \tag{15}$$

$$Viscosity Ratio : \lambda \equiv \frac{\mu_1}{\mu_2} \tag{16}$$

3. SOLUTION METHOD

The flow domain for each set of parameter values is unknown a priori, due to the presence of the liquid-liquid interface. In order to solve this free boundary problem by means of standard techniques for boundary value problems, the set of differential equations and boundary conditions posed in the unknown domain has to be transformed into an equivalent set, defined in a known reference domain. This transformation is made by a mapping $\underline{x} = \underline{x}(\xi)$ that connects the two domains as illustrated in Fig. 2. The unknown physical domain is parametrized by the position vector $\underline{x}$, and the reference domain by ξ. The mapping used here is the one presented by de Santos (1991), who showed that a functional of weighted smoothness can be used successfully to construct the type of mapping involved here. The inverse of the mapping that minimizes the functional is governed by a pair of elliptic differential equations identical to those governing diffusional transport with variable diffusion coefficients. The coordinates j and h of the reference domain satisfy

$$\nabla \cdot [D_\xi \nabla \xi] = 0 \tag{17}$$

$$\nabla \cdot [D_\eta \nabla \eta] = 0 \tag{18}$$

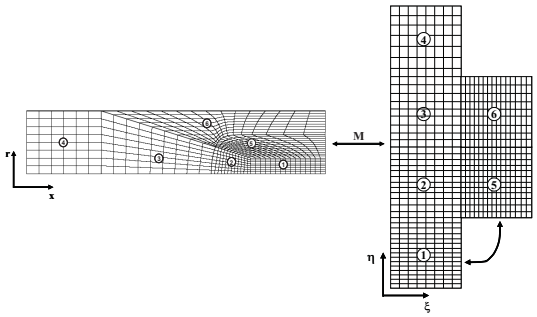

Figure 2. Mapping between the physical and reference domain.

Where D_ξ and D_η are diffusion coefficients used to control the element spacing.

Equations (17) and (18) describe the inverse mapping $\xi \equiv \xi(x)$. To evaluate $\xi \equiv \xi(x)$, the diffusion equations that describe the mapping also have to be transformed to the reference configuration. The gradient of mapping $\xi \equiv \xi(x)$ in a two-dimensional domain is defined as $\nabla_\xi x \equiv \mathbf{J}$. $||J|| = det\mathbf{J}$ is the Jacobian of the transformation.

In order to solve the second order partial differential equations. (17) and (18) boundary conditions are required. Along the solid walls and at the synthetic inlet and outlet planes, the boundary is located by imposing a relation between the coordinates x and r from the equation that describes the shape of the boundary, and stretching functions are used to distribute the points along the boundaries. The liquid-liquid interface is located by imposing the kinematic condition, Eq.(12).

The discrete version of the mapping equations are generally referred to as mesh generation equations. Spatial derivatives with respect to coordinates of the physical domain x can be written in terms of derivatives with respect to coordinates of the reference domain ξ by using the inverse of the gradient of the mapping:

$$\begin{bmatrix} \frac{\partial}{\partial x} \\ \frac{\partial}{\partial y} \end{bmatrix} = \mathbf{J}^{-1} \begin{bmatrix} \frac{\partial}{\partial \xi} \\ \frac{\partial}{\partial \eta} \end{bmatrix} \tag{19}$$

The differential equations that govern the problem were solved simultaneously with the aid of the finite element/Galerkin method. The velocity, pressure, and node position are represented in terms of basis functions

$$\mathbf{u} = \begin{bmatrix} u \\ v \end{bmatrix} = \begin{bmatrix} \sum_{i=1}^{n} U_j \phi_j \\ \sum_{i=1}^{n} V_j \phi_j \end{bmatrix} \tag{20}$$

$$\mathbf{p} = \sum_{i=1}^{m} P_j \, \chi_j \quad ; \quad \mathbf{x} = \sum_{i=1}^{n} X_j \, \phi_j \quad ; \quad \mathbf{r} = \sum_{i=1}^{n} R_j \, \phi_j \tag{21}$$

Biquadratic basis functions (ϕ_j) are used to represent the velocity and nodal coordinates and linear discontinuous functions (χ_j) to expand the pressure field. The coefficient of the expansions are the unknowns of the problem:

$\underline{c} = [U_j \quad V_j \quad P_j \quad X_j \quad R_j]^T$

The weighted residuals of the Galerking method are:

$$R^i_{mx} = \int_\Omega \left[\frac{\partial \phi_i}{\partial x} T_{(xx)k} + \frac{\partial \phi_i}{\partial r} T_{(xr)k} \right] r||J||d\Omega - \int_\Omega e_x (\mathbf{n} \cdot \mathbf{T}_k) \phi_i r \frac{d\Gamma}{d\Gamma} d\Gamma \tag{22}$$

$$R^i_{mr} = \int_\Omega \left[\frac{\partial \phi_i}{\partial x} T_{(xr)k} + \frac{\partial \phi_i}{\partial r} T_{(xr)k} + \frac{\phi}{r} T_{(\theta\theta)k} \right] r||J||d\overline{\Omega} - \int_\Omega e_r (\mathbf{n} \cdot \mathbf{T}_k) \phi_i r \frac{d\Gamma}{d\Gamma} d\Gamma \tag{23}$$

$$R^i_c = \int_\Omega \left[\frac{1}{r} \frac{\partial}{\partial r} (r v_k) + \frac{\partial u_k}{\partial x} \chi_i r||J||d\overline{\Omega} \right. \tag{24}$$

$$R^i_\xi = \int_\Omega D_\xi \left(\frac{\partial \phi}{\partial x} \frac{\partial \xi}{\partial x} + \frac{\partial \phi}{\partial r} \frac{\partial \eta}{\partial r} \right) ||J||d\overline{\Omega} + \int_\Gamma D_\xi (\nabla \xi \cdot \mathbf{n}) \phi_i \tfrac{d\Gamma}{d\Gamma} d\Gamma \tag{25}$$

$$R^i_\eta = \int_\Omega D_\xi \left(\frac{\partial \phi}{\partial x} \frac{\partial \eta}{\partial x} + \frac{\partial \phi}{\partial r} \frac{\partial \eta}{\partial r} \right) ||J||d\overline{\Omega} + \int_\Gamma D_\eta (\nabla \eta \cdot \mathbf{n}) \phi_i \tfrac{d\Gamma}{d\Gamma} d\Gamma \tag{26}$$

For elements located along the interface, the boundary integral of the residuals of momentum are calculated using Eq.(13). Once all the variables are represented in terms of the basis functions, the system of partial differential equations reduces to simultaneous algebraic equations for the coefficients of the basis function of all the fields. This set of equations is nonlinear and sparse. It was solved by Newtons method, and a quadratic convergence was obtained as the residual approached zero. The linear system of equations at each Newton iteration was solved using a frontal solver.

The overall domain length is equal to 15 inner diameters (L = 15D), the interface tip being located in the middle of it. The domain was divided into 6 regions, with a total of 651 elements that correspond to 2705 nodes and 12773 degrees of freedom. A representative mesh is shown in Fig. 3.

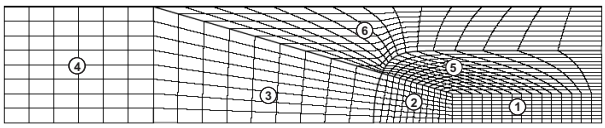

Figure 3. Finite element mesh with 651 elements and 12773 degrees of freedom.

4. RESULTS

The system of equations that governs the probleme is extremely non-linear. In order for Newtonŝ Method to converge, the initial guess needs to be close enough to the solution. The procedure used here was to first obtain a solution at intermediate capillary number, e.g. $Ca = 1$, and very low viscosity ratio, e.g. $\lambda = 1E^{-4}$. This corresponds to the case of a gas bubble displacing a viscous liquid. This initial case was used to validate the method, by comparing the predictions with the experimental results of Taylor. The thickness of the film attached to the capillary wall is expressed in terms of the mass fraction, as reported by Taylor, and defined by Eq. (1). The results are presented in Fig. 4. The agreement is excellent over the range of capillary number tested. Pseudo arc-length continuation was used to obtain solutions of the range of capillary numbers and viscosity ratio of interest. In order to validate the code to cases of finite values of viscosity ratio, the theoretical predictions were obtained at the same parameters of some of the experimental data reported by Mason (1). The comparison is shown in Tab 1. Again, agreement is excellent.

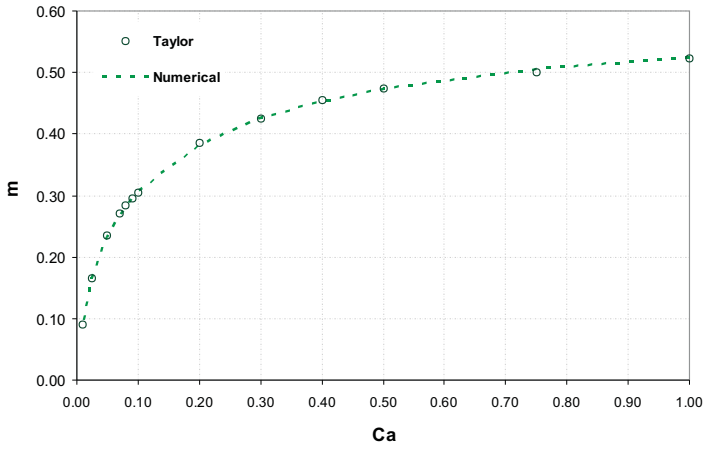

Figure 4. Comparison between experimental results of Taylor and the numerical prediction of present job for λ = $1E^{-4}$.

Table 1. Experimental Values (Goldsmith Mason) and numerical results of the present job for the film thickness h/R

Ca	λ	$h/R\ Mason$	$h/R\ Present\ Job$
1,296	1,08	0,483	0,478
0,599	1,08	0,605	0,597
0,095	6,00	0,766	0,756

Soares et al (2005) showed that, for the case of a less viscous liquid displacing a non-viscous liquid, the thickness of the film attached to the capillary wall rises as the viscosity of the drop increases. The tendency is the same for the cases at which the drop viscosity is larger than the continuos phase viscosity, as shown in Fig 5. The plot shows how the thickness of the liquid film in units of capillary radius changes with capillary number and viscosity ratio. As in the case of a gas displacing a viscous liquid, the thickness of the film left on the wall rises with capillary number. At low capillary number the effect of viscosity ratio on the film thickness is weak. At higher capillary numbers the thickness between the drop and the wall rises as the viscosity of the drop increases. The evolution of the streamlines near the drop tip as the viscosity ratio rises at $Ca = 0.001$ is shown in Fig 6. In all the cases, there is a small recirculation attached to the tip of the drop.

The influence of viscosity ratio, λ, in the film thickness for the liquid -liquid displacement in a capillary is analized. Fig. 5 shows the film thickness between the wall and the drop, h, as a function of the capillary number Ca, for three different viscosity ratios λ. It can be noted film thickness increases as viscosity ratio increases, in agreement with previous experimental results, as shown in Table 1.

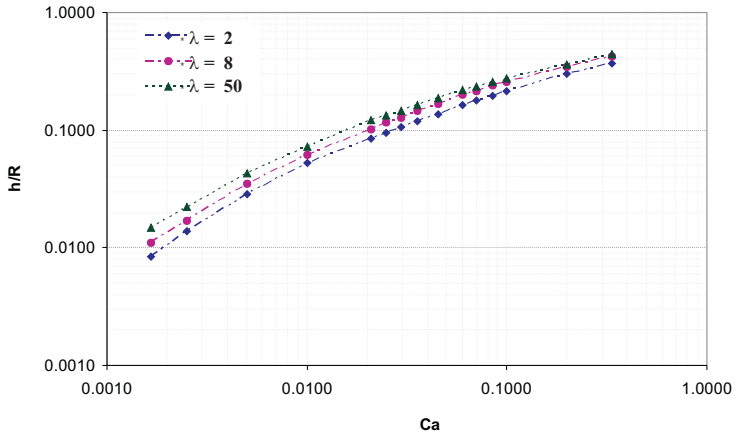

Figure 5. Film thickness as function of capillary number.

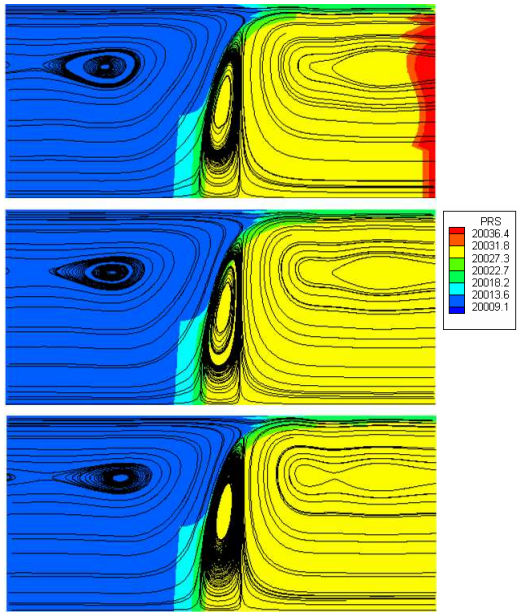

Figure 6. Streamlines for $Ca = 0.005$ and viscosity ratios λ of 2, 8 and 50.

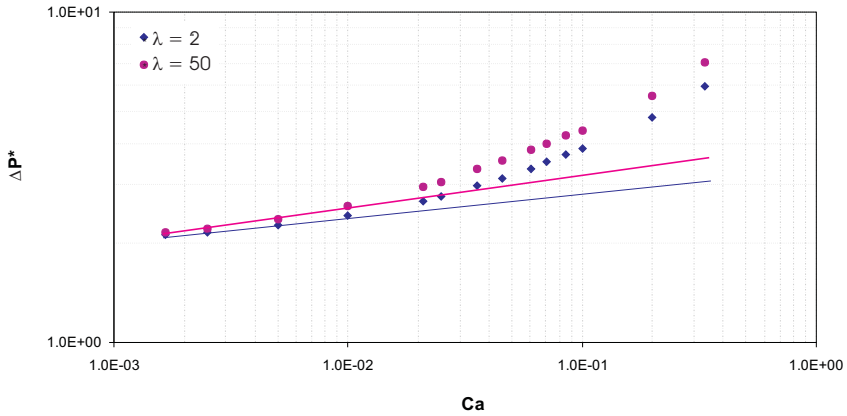

Figure 7. Non-dimensional drop pressure as a function of Ca for λ = 2 e 50. Assymptotyc lines with slopes of 42.4 and 60.3 respectively.

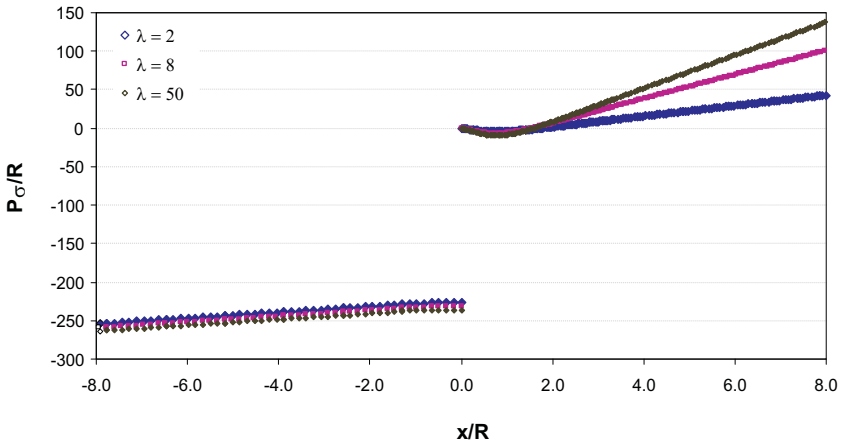

Figure 8. Pressure as a function of the position for viscosity ratios of λ = 2, 8 e 50 and $Ca = 0.005$.

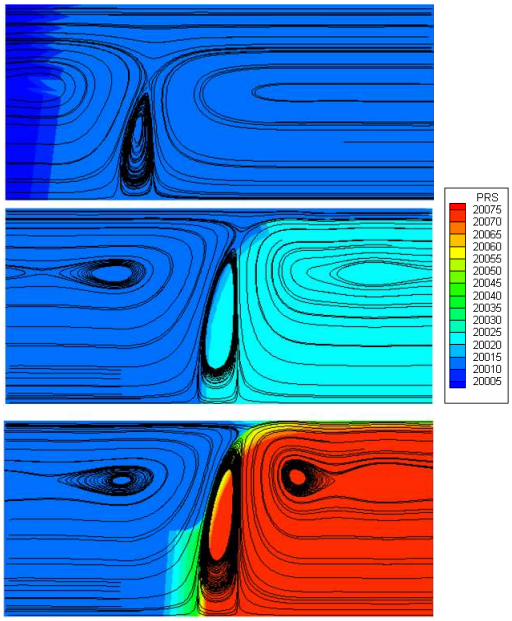

Figure 9. Streamlines for λ = 2 and capillary numbers Ca of 0.1, 0.01, and 0.0017.

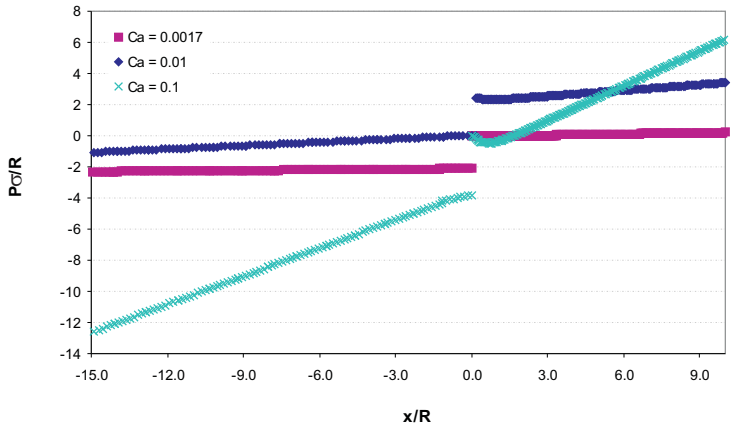

Figure 10. Pressure as a function of the position for λ = 2.

An important information to the complete understanding of flow of oil-water emulsions in porous media is to determine the flow-rate pressure drop relation as a function of the operating variables. Figure 7 shows the dimensionless pressure drop $\Delta P^* = \frac{\Delta P R^2}{\sigma L}$ as a function of the capillary number Ca and viscosity ratio. As expected, the pressure drop rises as the drop velocity increases. The effect of the drop viscosity on the pressure drop is weak. At Ca = 0.1, the pressure drop increases by only 5%, as the viscosity ratio rises from $\lambda = 2$ to $\lambda = 50$. The drop flows through the capillary lubricated by the thin film is left between the capillary wall and the interface.

It is important to observe the effect of discontinuity of the normal stress at the interface. Fig. 8 shows the pressure as a function of position x for $Ca = 0.005$. For effects of comparison, the point of the tip of interface (at simmetry line) is put as a referential for the pressure of both liquids, so $P^* = P(x) - P_d$, where P_d is the pressure at the tip of the interface. There is a neglictible change in extra pressure at the interface for different viscosity ratios. As expected the drop pressure as position x is increased is bigger for fluid 1 when viscosity is increased. There is a fall in the zone of the drop, before it rises, and this fall is bigger as more viscois is the drop.

The effect of capillary number on the flow patterns is now analyzed. For effect of comparison it is taken the case with viscosity ratio equal 2.

Figures 9 show streamlines of the flow with liquid-liquid interface for a Capillary number range of $0.0017 < Ca < 0.1$. As the capillary number decreases number of recirculations increases near the tip of the interface. Also, as the capillary number is reduced the size of the recirculation at tip of interface is bigger.

The effect of discontinuity of the normal stress at the interface is studied. Fig. 10 shows the pressure as a function of position x for $Ca = 0.005$. It can be observed that the extra pressure due to the presence of the interface depends upon the capillary number and this parameter is dominant over the viscosity ratio.

5. FINAL REMARKS

Immiscible displacement in capillaries is of great importance for many technological applications, including enhanced oil recovery.

Here, an axisymmetric model for the immiscible liquid-liquid displacement in a capillary tube was presented. Presence of fluid- fluid interface can strongly affect the problem complex, since the domain in which the differential equations are integrated is unknown a priori. A fully coupled formulation was used and the differential equations were solved via the Galerkin finite element method. The numerical predictions were confronted with experimental data available in literature and a good agreement was observed.

Works are found in the literature which analyze liquid displacement in tubes. Some of them are limited to gas-liquid displacement or to liquid-liquid displacement at rather small capillary numbers and scarce experimental works are found for the case when viscosity ratio is bigger than one. Numerical report for these last case are apparently absent in literature and experimental results are puntual.

The main contribution of the present work was the study of liquid-liquid displacement for the case of viscosity ratios bigger than 1, and the the capillary numbers obtained commonly in oil recovery process, which is the motivation of present job.

The predictions obtained here for the mass fraction for the case of viscotity ratio of the order $1E^{-4}$ agree quite well with experimental data of Taylor. For values of the viscosity ratio of the order of O(1), the theoretical predictions were compared with the experimental data reported by Goldsmith and Mason (1963), and good agreement was obtained. Experimental results for viscosity ratio of the O^1 is scarce, so experimental results regarding these cases would be more than welcome.

The analysis of the capillary number effect shows the number of recirculations increase near the tip of the interface as the capillary number is reduced and the size of the recirculation at tip of interface is bigger. The number of recicurlation increases in both liquids when viscosity ratio is increased. It is seen that film thickness increases as the viscosity ratio and capillary number is is increased.

Results obtained for the extra-pressure due to the presence of the interface points out that pressure gradient changes ahead of the tip of the interface by changing the capillary number while the effect of viscosity ratio is neglictible in this area. On the other hand, there is a fall in the zone of the drop, before it rises, and this fall is bigger as more viscous is the drop.

Results obtained are being used as excellent initial condition for the case of the liquid-liquid flow through a capillary with a constriction.

6. ACKNOWLEDGEMENTS

Sygifredo Cobos is sponsored by the Human Resources Program of PRH-ANP/MCT of the Petroleum National Agency of Brazil.

7. REFERENCES

Fairbrother, F., and Stubbs, A.E.,1935, "Studies in Electroendosmosis.Part VI. The bubble-Tube Methods of Measurement", J. Chem. Soc, Vol 1, pp. 527-529.

Goldsmith, H.L. and Mason, S.G.,1963, "The Flow of suspensions through tubes II. Single Large Tubes", Journal of Colloid Science, Vol. 18, pp.237-261.

Janssen, P., 2000, "Characterization of oil in water mixtures produced in high-watercut oil wells",PhD. Thesis.

Olbricht, W.L., 1996, "Pore-Scale prototypes of multiphase flow in porous media",Annu. Rev. Fluid. Mech, Vol.28, pp. 187-213.

Soares, E.J., Carvalho, M.S. and Souza Mendes P.R.,2005, "Immiscible Liquid-Liquid Displacement in Capillary tubes", Journal of Fluids Engineering, Vol. 127, pp.24-31.

Taylor, G.I., 1960, "Deposition of a viscous fluid on the wall of a tube", Journal of Fluid Mechanics, Vol.10, pp. 161-165.

8. Responsibility notice

The author(s) is (are) the only responsible for the printed material included in this paper